Ag Coated Microneedle Based Surface Enhanced Raman Scattering Probe for Intradermal Measurements

Clement Yuen[a], Quan Liu*[a]
[a] Division of Bioengineering, School of Chemical and Biomedical Engineering, Nanyang Technological University, 70 Nanyang Drive, Singapore 637457, Singapore

*email: quanliu@ntu.edu.sg; phone: +65 6316 8748; fax: +65 6791 1761

ABSTRACT

We propose a silver coated microneedle to detect test molecules, including R6G and glucose, positioned at a depth of more than 700 μm below a skin phantom surface for mimicking intradermal surface-enhanced Raman scattering measurements.

Keywords: Spectroscopy; Raman scattering; Biosensors; Nanostructured materials; Microstructure

1. INTRODUCTION

Capillary blood, dendritic cells and other human intradermal components have clinical importance in the areas of immunology, and diagnosis [1]. Among those methods, e.g. magnetic resonance imaging and fluorescence spectroscopy, that have been employed to analyze the human intradermal layer, Raman spectroscopy promises to provide information on chemical structures, conformations, and processes in biomolecules [2]. Although human skin can be characterized by Raman spectroscopy, measurements at a depth beyond 700 μm under the skin surface are difficult partially because the Raman signal of biomecules is weak [2, 3]. In contrast, Raman signal can be augmented up to 10^{14} folds in the surface-enhanced Raman scattering (SERS) strategy for test molecules in close vicinity to a metal surface [e.g., silver (Ag) and gold] [3], but the subcutaneous injection of nanoparticles required in typical *in vivo* SERS measurements can be toxic to human body. Recently, pain reduction has been demonstrated in the administration of microneedles for intradermal drug delivery [4]. Therefore, we propose an Ag-coated microneedle-based SERS probe to detect test molecules buried (more than 700 μm) inside tissue-like phantoms that mimic the scattering and absorption properties in human skin.

2. MATERIALS AND METHODS

2.1 Preparation of silver (Ag) coated microneedle

A layer of 750-nm thick Ag film was coated onto microneedle patches (AdminPatch® 1200 [4], Admin-Med). Tollen's method was employed to fabricate the Ag films because Ag films synthesized by this method in other substrates [5] have shown effective SERS at 785-nm excitation. The microneedle patch was positioned inside a mixture of 0.3 M $AgNO_3$ in a volume of 1.5 ml and 2.5 M NaOH in a volume of 0.75 ml. Next, 0.2 ml NH_4OH at a concentration of 28 % w/w was added drop by drop to dissolve the precipitates formed. Finally, Ag ions were reduced to form the Ag film by introducing 4.5 ml of glucose at a concentration of 0.1 M. The microneedle was taken out after 15 minutes, rinsed with deionized water and dried up prior to testing. For the detection of glucose, the microneedle was incubated with 1-decanethiol (1mM) in ethanol for 16 hours prior to SERS measurements.

2.2 Synthesis of phantom layers

Figure 1 shows the experimental setup for the synthesis of the agarose phantom layers. A 1 % agarose solution was boiled. When the agarose solution was cooled to about 60 °C, this solution was mixed with nigrosin at a concentration of 6 μM and intralipid-20% in a volume of 1.967 ml, to give a total volume of 50 ml. Nigrosin was added as an absorber and intralipid was introduced as an elastic scatterer, for mimicking the absorption and scattering properties of the human skin [6]. The mixture was set within a 760-μm gap, which was formed between two glass slides sandwiched between four cover slips [Fig. 1(a) and 1(b)]. The same procedures were employed to synthesize the bottom layer. Test molecules,

Clinical and Biomedical Spectroscopy and Imaging III, edited by Volker Deckert, Nirmala Ramanujam,
Proc. of OSA Biomedical Optics-Vol. 8798, 87980R · © 2013 OSA-SPIE
CCC code: 1605-7422/13/$18 · doi: 10.1117/12.2032513

Rhodamine 6G (at concentrations ranging of 10^{-2} and 10^{-4} M) and glucose (at concentrations ranging from 0 to 150 mM) were introduced together with the aforesaid absorbers and scatterers at about 60 °C prior to setting in a Petri dish.

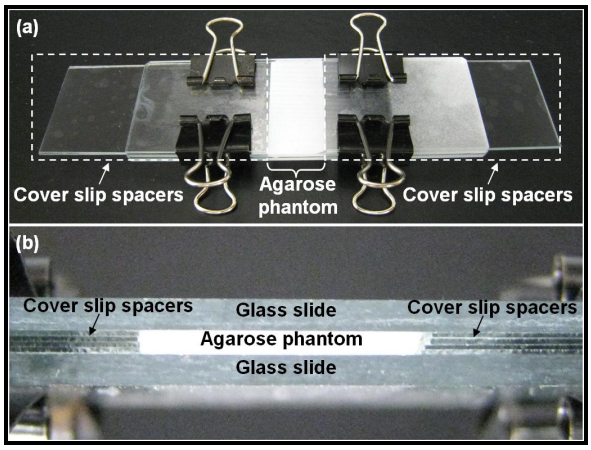

Figure 1. (a) Top oblique and (b) view of the experimental setup for the synthesis of the 760-μm top agarose phantom layer.

2.3 Raman instrumentation

In SERS measurements, the 760-μm top layer was stacked on the bottom layer. The Ag-coated microneedle patch was pressed onto the top phantom layer and pierced into the bottom phantom layer. All samples were analyzed by using an inVia Renishaw Raman system with 785-nm excitation wavelength. An excitation power of 5 mW was employed for SERS measurements and 100 mW for the ordinary Raman measurements of R6G and glucose at different concentrations.

3. RESULTS AND DISCUSSIONS

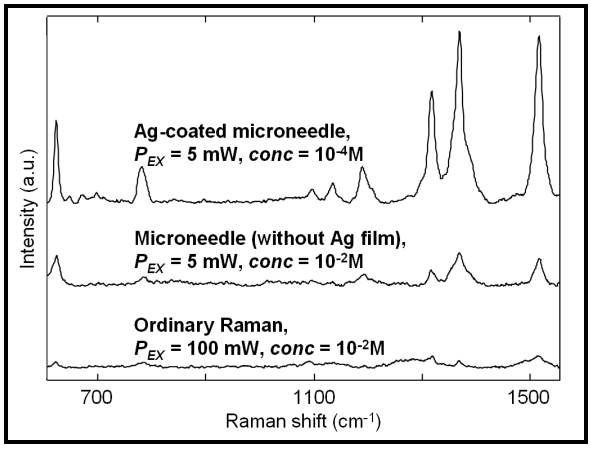

Fig. 2. SERS spectra of R6G buried inside phantoms at 760 μm below the surface measured by using Ag-coated microneedle (R6G concentration: 10^{-4} M; P_{EX}: 5 mW), microneedle (R6G concentrations: 10^{-2} M; P_{EX}: 5 mW), and the ordinary Raman spectrum (R6G concentrations: 10^{-2} M; P_{EX}: 100 mW). P_{EX} means the excitation power and *conc* means R6G concentration.

Figure 2 gives the Raman spectra of R6G buried in the bottom phantom layer at 760 μm below the surface measured by Ag-coated microneedle and microneedle without Ag coating, in comparison to the ordinary Raman spectrum acquired without the microneedle. Prominent Raman peaks located at about 615 cm^{-1} (C–C–C ring in-plane bending), 775 cm^{-1} (CH out-of-plane bending), 1185 cm^{-1} (C–O–C stretching), 1310 cm^{-1} (C–C/C–N stretching), 1365 cm^{-1} (C–C/C–N stretching), and 1508 cm^{-1} (aromatic C–C stretching)[7], are noted in the R6G Raman spectra measured using the microneedle based SERS probe. In contrast, the ordinary Raman spectra of R6G at a higher concentration of 10^{-2} M show only weak Raman peaks even with a higher excitation power of 100 mW.

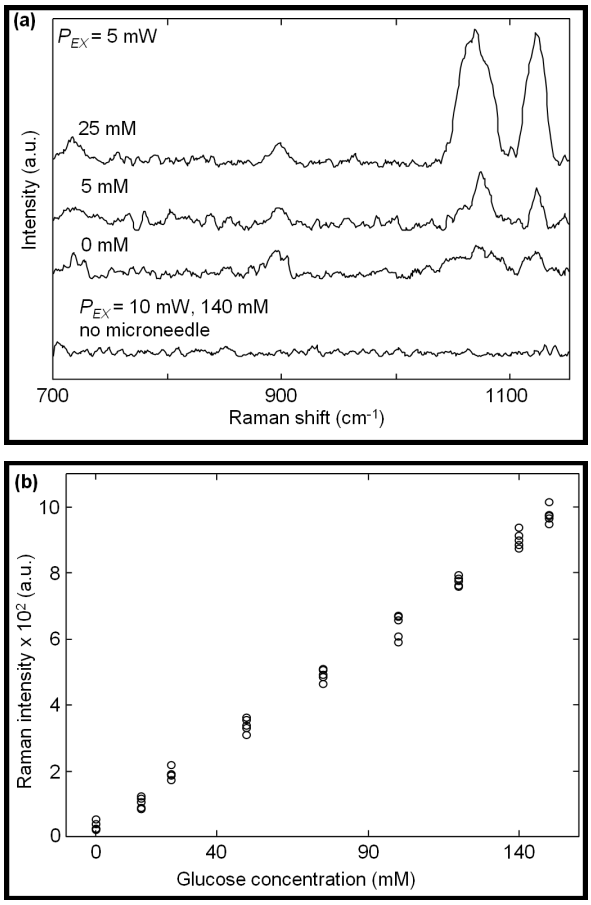

Fig. 3. (a) SERS spectra for the glucose concentrations of 0, 5, and 25 mM positioned inside phantom at 760 μm below the surface measured by using the Ag-coated microneedle-based probe at an excitation power of 5 mW, and ordinary Raman of glucose phantom at concentration of 140 mM without microneedle at an excitation power of 10 mW. (b) SERS intensity at 1124 cm^{-1} (C–O–H deformation) of glucose inside the two-layered phantom at concentrations ranging from 0 to 150 mM.

Figure 3 shows the SERS spectra and the dependence of the SERS intensity at 1124 cm^{-1} of glucose buried inside the bottom phantom layer at a depth of 760 μm below the surface measured by using the Ag-coated microneedle-based probe. Prominent Raman peaks are noted at about 1076 (C–C) and 1124 cm^{-1} (C–O–H deformation) [8], in the SERS spectra of glucose measured by our proposed probe [Fig. 3(a)]. Conversely, these peaks cannot be observed for the ordinary Raman measured without the microneedle. Raman intensities increase linearly with the increment in glucose concentrations [Fig. 3(b)], in contrast to the unchanged Raman intensity peaks at 714, 889, 1073 and 1128 cm^{-1} [Fig. 3(a)], which are attributed to the 1-decanethiol adsorbed on the Ag-coated surface that give the non-zero intercept for glucose concentration at 0 mM [Fig. 3(b)].

4. CONCLUSIONS

In conclusion, our porposed Ag-coated microneedle-based SERS probe can detect test molecules buried at a depth of more than 700 μm inside a two-layered phantom that mimics the human skin. This strategy also quantifies glucose concentrations, which demonstrates its potential for in vivo SERS intradermal SERS measurements.

5. ACKNOWLEDGEMENTS

This research was funded by the Singapore Lee Kuan Yew (LKY) start-up grant and the New Investigator Grant (Project No. NMRC/NIG/1044/2011) funded by the National Medical Research Council (NMRC) in Singapore.

6. REFERENCES

[1] Borys, N. J., and Lupton, J. M., "Surface-enhanced light emission from single hot spots in Tollens reaction silver nanoparticle films: Linear versus nonlinear optical excitation," J. Phys. Chem. C, 115(28), 13645-13659 (2011).

[2] Dam, J. S., Pedersen, C. B., Dalgaard, T., Fabricius, P. E., Aruna, P., and Andersson-Engels, S., "Fiber-optical probe for noninvasive real-time determination of tissue optical properties at multiple wavelengths," Appl. Opt., 40(7), 1155-1164 (2001).

[3] Keren, S., Zavaleta, C., Cheng, Z., Zerda, A., Gheysens, O., and Gambhir, S. S., "Noninvasive molecular imaging of small living subjects using Raman spectroscopy," Proc. Natl. Acad. Sci., 105(15), 5844-5849 (2008).

[4] Krafft, C., Dietzek, B., and Popp, J., "Raman and CARS microspectroscopy of cells and tissues," Analyst, 134(6), 1046-1057 (2009).

[5] Romani, N., Clausen, B. E., and Stoitzner, P., "Langerhans cells and more: langerin-expressing dendritic cell subsets in the skin," Immunol Rev., 234(1), 120-141 (2010).

[6] Vasko, P. D., Blackwell, J., and Koenig, J. L., "Infrared and Raman spectroscopy of carbohydrates. Part II: Normal coordinate analysis of α-D-glucose," Carbohyd. Res., 23(3), 407-416 (1972).

[7] Yuen, C., and Liu, Q. "Magnetic field enriched surface enhanced resonance Raman spectroscopy for early malaria diagnosis," J. Biomed. Opt., 17(1), 017005 (2012).

[8] Yuzhakov, V. V., "The adminpenTM microneedle device for painless and convenient drug delivery," Drug Deliv. Technol., 10(4), 32-36 (2010).